

# Micro- or nanoseparated phases in thermoset blends of an epoxy resin and PEO–PPO–PEO triblock copolymer

M. Larrañaga<sup>a</sup>, N. Gabilondo<sup>a</sup>, G. Kortaberria<sup>a</sup>, E. Serrano<sup>a</sup>, P. Remiro<sup>a</sup>, C.C. Riccardi<sup>b</sup>,  
I. Mondragon<sup>a,\*</sup>

<sup>a</sup>*Materials and Technologies Group, Dpto. Ing. Química y M. Ambiente, Escuela Univ. Politécnica, Universidad del País Vasco/Euskal Herriko Unibertsitatea, Pza. Europa, 1, 20018 Donostia-San Sebastián, Spain*

<sup>b</sup>*Institute of Materials Science and Technology (INTEMA), University of Mar de Plata and National Research Council (CONICET), J.B. Justo 4320-7600 Mar de Plata, Argentina*

Received 8 October 2004; received in revised form 1 April 2005; accepted 13 May 2005

Available online 17 June 2005

## Abstract

Diaminodiphenylmethane (DDM) curing at several temperatures of a diglycidyl ether of bisphenol A (DGEBA) epoxy resin modified with a poly(ethylene oxide)-*block*-poly(propylene oxide)-*block*-poly(ethylene oxide) (PEO–PPO–PEO) block copolymer has been investigated in order to characterize the miscibility and morphological features. Two distinct phases are present for every blends studied except for DGEBA/DDM modified with 10 wt% PEO–PPO–PEO and cured at low temperature. Depending on the curing condition, phase separation takes place at micro or nanoscale due to competition among kinetic and thermodynamic factors. The mechanistic approach used for modeling the curing reactions shows that the formation of epoxy–hydroxyl complex and the auto catalytic process are slightly decreased whilst the noncatalytic process is favoured upon copolymer addition. Modifier addition delays curing process as the influence of both formation of epoxy–hydroxyl complex and catalytic process on reaction rate is higher than the influence of noncatalytic process. A thermodynamic model describing a thermoset/block copolymer considered as only one entity system is proposed. The LCST behaviour allows to elucidate nano or micro separated structures obtained at low and high curing temperatures, respectively.

© 2005 Elsevier Ltd. All rights reserved.

*Keywords:* Epoxy modification; Triblock copolymer; Phase separation

## 1. Introduction

The importance on control of structure formation of materials has increased, specially on the nanometer scale, because of their potential applications as membranes, catalyst supports, materials with photonic crystals properties, etc. [1–3]. Epoxy-based thermosets have been modified with rubbers or thermoplastics to improve their fracture toughness. Polymers typically added in epoxy systems are homopolymers [4,5] or random copolymers [6,7], which give different microstructures (particulate, co-continuous) depending on percentage and type of polymer and curing temperature as well. However, only few works have been performed with nanostructured thermosets [8–14]. A

recent trend is to incorporate block copolymers able to undergo self-assembling to obtain nanoscale structures. Block copolymers have received considerable attention, both experimentally and theoretically, due to their fascinating ability to self-assemble into a variety of ordered nanoscale morphologies. Thus, after adding the hardener for epoxy curing, depending on the curing conditions, different nanomorphologies can be withheld in blends with block copolymers. The first work to report ordered nanostructures on thermosets modified with block copolymers is addressed in 1997 by Hillmyer et al. [1]. They studied blends of poly(ethylene oxide)-*block*-poly(ethyl ethylene) (PEO–PEE) or poly(ethylene oxide)-*block*-poly(ethylene-*alt*-propylene) (PEO–PEP) copolymers with diglycidylether of bisphenol-A (DGEBA) and an aromatic curing agent [1,2,8]. The copolymers consisted of an epoxyphobic alkane block and another poly(ethylene oxide) (PEO) block, which is miscible with DGEBA. Materials exhibited nanoordered morphologies in both uncured and cured states.

\* Corresponding author. Tel.: +34 943017163; fax: +34 943017130.

The same group also introduced block copolymers with reactive epoxy groups [9]. Poly(ethylene oxide)-*block*-poly(ethylene) (PEO-PE) copolymer has also been used to modify DGEBA [10]. Mijovic et al. [11] studied the modification of an epoxy resin with PEO-PPO-PEO block copolymer by dielectric relaxation spectroscopy (DRS), differential scanning calorimetry (DSC) and atomic force microscopy (AFM). They observed microscopic separation in selected conditions. However, Guo et al. [12] obtained nanostructured blends for the same composition even though the triblock copolymer used had high molecular weight. This discrepancy seems to be related with the different curing conditions used as well as to the inner characteristics of the block copolymer.

The present study discusses morphological variations in DGEBA/DDM (4,4'-diaminodiphenylmethane) epoxy blends modified with several amounts of PEO-PPO-PEO block copolymer. Several curing temperatures have been used. A mechanistic approach for curing kinetics and thermodynamic modelling of phase separation are reported with the purpose to explain the morphologies. The thermodynamic model developed considers the block copolymer as only one entity. Morphological behaviour has been investigated by atomic force microscopy (AFM), results being compared with those obtained by dynamic mechanical analysis (DMA).

## 2. Experimental

The epoxy resin used was DER-332, a DGEBA resin kindly supplied by Dow Chemical, with an epoxy equivalent weight of around 175 g/equiv and a hydroxyl/epoxy ratio close to 0.03. The curing agent was DDM (HT-972), kindly supplied by Ciba, with an amine equivalent weight of 49.5 g/equiv. The modifier was PEO-PPO-PEO block copolymer from Polysciences, with molecular weight  $M_w=2900$  g/mol and an overall molar ratio between blocks 2PEO:PPO of 0.8:1. Homopolymers such as PEO  $M_w=8000$  g/mol and PPO  $M_w=2000$  g/mol have also been investigated. The amine-to-epoxy ratio for DGEBA/DDM system was 1.0 in all blends. The content of modifier has been varied from 0 to 30 wt%.

Molecular weight distributions of PEO-PPO-PEO were measured by Perkin-Elmer S-250 gel permeation chromatography (GPC), equipped with a Perkin-Elmer LC-235 UV detector set at 245 nm and a refractive index detector LC-30 RI, and using three Waters styragel columns, HR 2, HR 4 and HR 5E, whose molecular weight range detection was 500–20,000, 5000–500,000 and 2000–4,000,000, respectively. The mobile phase was tetrahydrofuran (THF) at a flow rate of 1 mL/min and 25 °C. Calibration was performed using polystyrene standards due to absence of Mark-Houwink constants for these block copolymers in THF. The number and weight average molecular weights were 3540 and 4220 g/mol, respectively, being the polydispersity

index of 1.19. These values are slightly different to those reported by Polysciences since they are referred to PS standards.

Samples were prepared in the following way. First, PEO-PPO-PEO was added to DGEBA at 80 °C and stirred for mixing. Then DDM was added in a stoichiometrical amount with continuously stirring in an oil bath at 80 °C for approximately 5 min, until a homogeneous blend was achieved. Blends were cured in a preheated mold and degassed with vacuum during the early stage of curing. Two curing cycles were employed, 80 °C for 6 h and 140 °C for 3 h. Samples were post-cured at 190 °C for 2 h, allowing them to cool gradually to room temperature.

Differential scanning calorimetry (DSC) measurements were performed with a Perkin-Elmer DSC-7 for the analysis of curing kinetics. For calibration high purity indium was used. All experiments were conducted under a nitrogen flow of 20 cm<sup>3</sup>/min, working with 5–7 mg samples in aluminium pans. Isothermal curing was carried out at several temperatures (80, 100, 120, 140, 150, 160 and 170 °C). After thermograms levelled off to the baseline, all samples were rapidly cooled. Then a dynamical DSC scan from 35 to 250 °C at 10 °C/min was performed to determine the residual heat of reaction ( $\Delta H_{res}$ ). The conversion of each sample  $x$  under isothermal conditions was calculated as the ratio of the partial reaction heat over total reaction heat,  $x=(\Delta H_{iso})_t/((\Delta H_{iso})+(\Delta H_{res}))$ , where  $(\Delta H_{iso})_t$  is the enthalpy of reaction at a time  $t$  obtained from the isothermal measurement, and  $(\Delta H_{iso})+(\Delta H_{res})$  is the sum of the total enthalpy from the isothermal ( $\Delta H_{iso}$ ) and the residual measurements.

Glass transition temperatures ( $T_g$ ) of blends were measured by dynamical scans from –100 to 50 °C at 20 °C/min, taken as the onset point of the step in the heat flow.

Transmission optical microscopy (TOM) measurements were made using an Olympus BH-2 optical microscopy equipped with a Mettler EP2HF heating stage. Samples were placed between a glass microscope slide and a glass cover. Cloud point times  $t_{cp}$  were determined as the time at which a decrease in the transmitted light intensity was recorded.

The morphology of tested samples was studied by atomic force microscopy (AFM) with a scanning probe microscope (SPM) (Nanoscope IIIa, Multimode™ from Digital Instruments) operating in tapping mode under ambient conditions. Etched silicon probes with a cantilever configuration of single beam and 125 μm of length and a tip with a nominal radius of curvature of 5–10 nm were used.

Dynamic mechanical properties were analysed in a Metravib viscoanalyser from 30 to 250 °C at 3 °C/min and 10 Hz using 60×12×5 mm<sup>3</sup> samples with a bending device. A constant amplitude of 0.1 V was employed. An initial displacement of 80 μm was applied to ensure contact between sample and geometry.

### 3. Results and discussion

DSC measurements were carried out in order to investigate the miscibility of PEO–PPO–PEO block copolymer with DGEBA/DDM blend. Fig. 1 shows thermograms of individual components and 20 wt% modified systems before curing. PPO is an amorphous polymer with a  $T_g$  of  $-73^\circ\text{C}$ . Unreacted DGEBA/DDM blend presents a  $T_g$  of  $-16^\circ\text{C}$ . Initially transparent DGEBA/DDM/PPO blend becomes opaque during curing as phase separation process takes place. It is worth noting that a single  $T_g$  around  $-27^\circ\text{C}$  is detected for the uncured blend, confirming that blends are initially miscible. The block copolymer used in this study shows the  $T_g$  at  $-71^\circ\text{C}$  (only one  $T_g$  is present due to the  $T_g$ s of both blocks are very close [11,12]) and the melting point at around  $-5^\circ\text{C}$ , taken at the onset of the melting. The blend modified with 20 wt% PEO–PPO–PEO shows a single  $T_g$  at around  $-25^\circ\text{C}$ , close to the value of system modified with PPO. Thus PEO–PPO–PEO was also initially miscible with epoxy system.

Indeed, as it is shown below, morphology of the modified epoxy blends after curing is a result of phase separation from an initial homogeneous miscible blend to a final different state: miscible, nanoseparated or microseparated. Phase separation process is controlled by thermodynamic and kinetic factors. For a better understanding of different morphologies obtained, before analyzing microstructures of DGEBA/DDM/PEO–PPO–PEO blends, both thermodynamics of phase separation and kinetics of curing of blends were investigated for several PEO–PPO–PEO contents.

#### 3.1. Kinetics of curing

In a previous work, the influence of temperature and

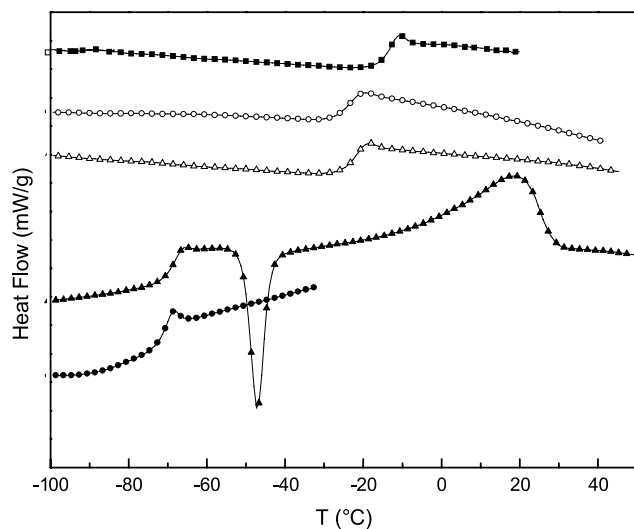


Fig. 1. DSC thermograms of (●) PPO, (▲) PEO–PPO–PEO and unreacted DGEBA/DDM systems for: (■) neat epoxy, (○) 20 wt% PPO, and (△) 20 wt% PEO–PPO–PEO.

block copolymer content on the kinetics of curing was studied [15]. Figs. 2 and 3 show the influence of these variables on conversion–curing time plots. As it is shown, the increase of copolymer content clearly delays curing reactions whilst the reaction rate increases with curing temperature.

In this work, different reactivities of primary and secondary amine hydrogens have been incorporated to the reaction scheme previously reported by Riccardi et al. [16]. The mechanistic approach used takes into account the following curing steps: epoxy activation by hydrogen bonding with hydroxyl groups in the pre-equilibrium to form an epoxy–hydroxyl complex, uncatalyzed addition reactions of primary and secondary amine hydrogens with epoxy groups, and parallelly, autocatalyzed reactions which take place due to the OH groups produced during curing reactions. Some researchers have also accounted for etherification reactions between epoxy and hydroxyl groups. However, as suggested by Girard-Reydet et al. [17], these reactions can be neglected for stoichiometric blends, above all at low curing temperatures.

The corresponding kinetic model, assuming different reactivities of primary and secondary amine hydrogens, is:

$$\frac{dx}{dt} = [K_1'(1-x-y) + K_1y] \left[ \frac{2(1-r)z_1 + rz_1^{r/2}}{2-r} \right] \quad (1)$$

$$\frac{dz_1}{dt} = -2z_1[K_1'(1-x-y) + K_1y] \quad (2)$$

where

$$y = 0.5 \left\{ A - [A^2 - 4[C_0 + x(1-C_0) - x^2]]^{0.5} \right\} \quad (3)$$

$$A = 1 + C_0 + \frac{1}{K} \quad (4)$$

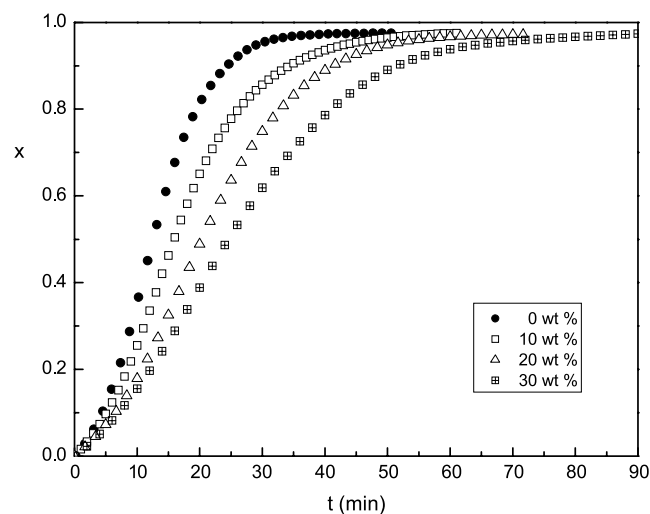


Fig. 2. Conversion vs. time curves of epoxy blends with several amounts of block copolymer cured at  $120^\circ\text{C}$ .

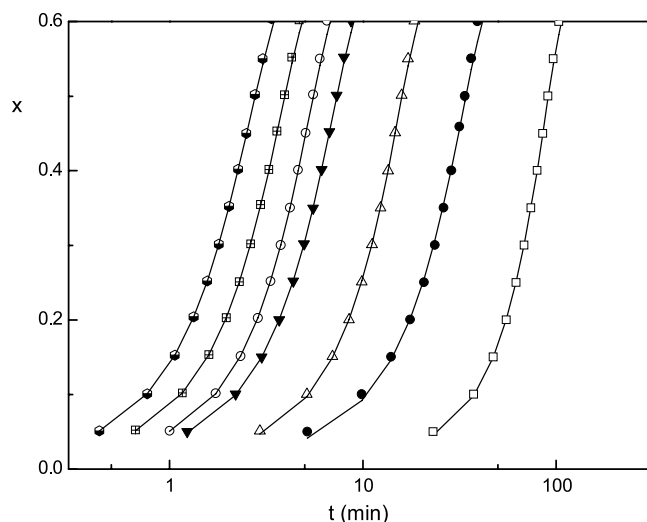


Fig. 3. Comparison between the mechanistic model (—) and experimental data at (□) 80 °C, (●) 100 °C, (△) 120 °C, (▼) 140 °C, (○) 150 °C, (■) 160 °C and (●) 170 °C for the blend modified with a 10 wt% block copolymer.

and

$$x = \frac{e_0 - [e + (e - \text{OH})]}{e_0} \quad (5)$$

$$z_1 = \frac{a_1}{e_0} \quad (6)$$

In these expressions  $e_0$  and  $e$  are the concentration of epoxy equivalents at time 0 and  $t$ , respectively;  $a_1$  is the concentration of primary amine hydrogens, and  $r$  is the ratio of secondary to primary amino-hydrogen rate constants. It was taken as 0.65, as Girard-Reydet et al. [17] determined.  $K$  is dimensionless equilibrium constant for epoxy–hydroxyl complex and  $K_1'$  and  $K_1$  are dimensionless kinetic constants for uncatalyzed addition reactions and autocatalyzed reactions, respectively;  $e\text{-OH}$  is the epoxy hydroxyl complex concentration.  $C_0$ , equiv OH/equiv epoxy, is 0.015 and  $y$  is  $e\text{-OH}/e_0$ . In Fig. 3, fits of experimental curves with kinetic model for 10 wt% modified system at different temperatures are shown. As it can be seen, the model provides good agreement with the experimental curves at the different curing temperatures analysed.

The rate constants determined for neat DGEBA/DDM are:

$$K = 1.07 \times 10^{-5} \exp\left(\frac{6283}{T}\right)$$

$$K_1 = 1.08 \times 10^6 \exp\left(-\frac{5889}{T}\right)$$

$$K_1' = 5.55 \times 10^5 \exp\left(-\frac{7438}{T}\right)$$

Values of the ratios of kinetic constants, represented as an average in the 80–170 °C range, and the initial ratio of the epoxy group concentrations in DGEBA/DDM/PEO–PPO–PEO blends and neat system are shown in Table 1. The addition of copolymer modifies the kinetic constants respect to the neat system.  $K$  and  $K_1$  constants slightly decrease as the copolymer content increases. Thus, the formation of epoxy–hydroxyl complex and the auto catalytic process are hindered by block copolymer adding. The constant for the uncatalyzed reaction of epoxy with amine increases with copolymer content. The addition of copolymer yields to dilution of the system, and thus the concentration of epoxy equivalents in initial blend decreases. If dilution of reactants would be the only factor determining the change on kinetic constants,  $K_{1\text{Blend}}/K_{1\text{Neat}}$  and  $K_{1\text{Blend}}'/K_{1\text{Neat}}'$  average values between 80 and 170 °C should be equal to  $e_{0\text{Blend}}/e_{0\text{Neat}}$  value. Thus the lower values observed can be explained taking into account that the OH groups formed in curing reactions interact by hydrogen bonding with the block copolymer [15,18]. The formation of epoxy–hydroxyl complex and the catalytic process are reduced. On the other hand, the increase of  $K_1'$  can be due to the fact that initially less epoxy groups interact with hydroxyl groups when block copolymer content is increased. As a consequence, more epoxy groups are available for direct reaction with amine.

Table 2 shows activation energies of different analysed systems. The activation energies for neat epoxy system are in reasonable agreement with those reported in the literature [19]. Modified systems present similar activation energies with respect to neat system. The influence of modifier can be seen in frequency factor values, which slightly decrease for auto-catalytic process whilst they increase for noncatalytic process. Indeed, even though the noncatalytic process is favoured in modified systems, the modifier delays reaction. That is to say that the influence of  $K$  and  $K_1$  constants on reaction rate is higher than the influence of  $K_1'$ .

### 3.2. Thermodynamic modeling

For all the compositions analyzed the copolymer is initially miscible with the epoxy system, but at a particular conversion, depending on the composition and reaction temperature, nano or micro phase separation take place. Experimental cloud-point times ( $t_{\text{cp}}$ ) were fitted to a thermodynamic model based on the Flory–Huggins (F–H) equation [20], which considers the polydispersity of each

Table 1  
Values of the ratios of kinetic constants and the initial ratio of the epoxy group concentrations in blends and neat system

PEO–PPO– PEO (wt%)	$K_{\text{Blend}}/K_{\text{Neat}}$	$K_{1\text{Blend}}/$ $K_{1\text{Neat}}$	$K_{1\text{Blend}}'/$ $K_{1\text{Neat}}'$	$e_{0\text{Blend}}/$ $e_{0\text{Neat}}$
10	0.75	0.72	1.86	0.89
20	0.68	0.55	1.98	0.79
30	0.60	0.43	2.23	0.68

Table 2  
Activation energy and frequency factor values of blends

PEO–PPO–PEO (wt%)	$E_1$ (kJ mol <sup>-1</sup> )	$E'_1$ (kJ mol <sup>-1</sup> )	$\ln(A_1'/[\text{min}^{-1}])$	$\ln(A_1'/[\text{min}^{-1}])$
0	49.0	61.8	13.9	13.2
10	49.7	62.1	13.8	13.9
20	49.7	62.3	13.5	14.1
30	49.7	62.5	13.3	14.2

blend component. This approach is similar to that used by Riccardi et al. [21] to describe a thermoset/thermoplastic system, being a first approach where the block copolymer is considered as only one entity. The blend to be described consists of a mixture of oligomeric epoxy-amine species (component 1) and a mixture of oligomeric species of PEO–PPO–PEO block copolymer (component 2).

F–H equation to describe the free energy of mixing of two polydisperse polymers per mole of unit cell is given by

$$\frac{\Delta G^m}{RT} = \sum \frac{\Phi_i}{Z_i} \ln \Phi_i + \sum \frac{\Phi_j}{Z_j} \ln \Phi_j + \chi \Phi_1 \Phi_2 \quad (7)$$

where  $R$  is the gas constant,  $T$  is the absolute temperature (K),  $Z_i = (V_i/V_r)$  and  $Z_j = (V_j/V_r)$  are the number of lattice sites occupied by  $i$ -mer (epoxy-amine specie) and  $j$ -mer (copolymer specie), being  $V_i$  and  $V_j$  the volume of the  $i$ -mer and  $j$ -mer, respectively, and  $V_r$  the reference volume taken as the volume for the smallest species (DDM). The volume fractions of reactive blend and copolymer are  $\Phi_1 = \sum_i \Phi_i$  and  $\Phi_2 = \sum_j \Phi_j$ , respectively, and  $\chi$  is the interaction parameter, which is taken to fit experimental cloud-point curves.

The molecular weight distribution of PEO–PPO–PEO was calculated experimentally by GPC (not shown here), which is necessary to know the volume of  $i$ -mer. The distribution of epoxy-amine species  $E_{m,n}$ , containing  $m$  DDM and  $n$  DGEBA molecules, at an overall conversion  $x$ , which is necessary to know the volume of  $j$ -mer, is given by the Stockmayer equation [22,23] (8), as shown by Riccardi et al. for other modified epoxy-amine systems [24]. Stockmayer equation assumes that  $r$  is 1. In spite of the fact that primary and secondary amines  $r$  is 0.65, the influence of this effect on the molar mass distribution can be neglected [21,25]. Thus the concentration of an  $E_{m,n}$  specie can be described as:

$$[E_{m,n}] = [A]_0 \frac{4(3m)!x^{m+n-1}(1-x)^{2m+2}}{m!(3m-n+1)!(n-m+1)!} \quad (8)$$

where  $[A]_0$  is the initial molar concentration of DDM in the blend. The volume fraction of an  $E_{m,n}$  specie is given by:

$$\Phi_{m,n} = [E_{m,n}][mV_{\text{DDM}} + nV_{\text{DGEBA}}] \quad (9)$$

and the volume fraction of component 1 is:

$$\Phi_1 = \sum_i \Phi_i = \sum_m \sum_n \Phi_{m,n} \quad (10)$$

By using cloud point times of the phase micro separated blends and curing kinetic curves, cloud point conversions can be obtained. These data allow knowing the molar concentration of  $E_{m,n}$  species at the cloud point time. These calculations are reported in detail by Riccardi et al. for similar systems in previous works [24,26].

Considering this thermodynamic model, the interaction parameter can be fitted as a function of conversion and temperature:

$$\chi = 3.25 - \frac{1.4 \times 10^3 - 2.15 \times 10^2 x}{T} \quad (11)$$

Cloud-point conversions  $x_{\text{cp}}$  at different curing temperatures for blends containing several amounts of PEO–PPO–PEO are shown in Fig. 4. Increasing the reaction temperature shifts  $x_{\text{cp}}$  downwards, which is typical for a LCST (lower critical solution temperature) behaviour [27]. This LCST behaviour can be observed in  $\chi$  expression, which is ( $a - (b/T)$ ) type [26], where  $a$  is the entropic contribution and  $b/T$  is the enthalpic part. The enthalpic contribution to the interaction parameter varies with conversion due to changes in the chemical structure of epoxy matrix and also to associated specific interactions,  $b = f(x)$ . The increase of  $\chi$  upon temperature leads to a less compatible system. So, in opposite to that observed for UCST behaviour [21], phase separation takes place at lower conversion as curing temperature increases.

Fig. 5 shows experimental cloud-point times  $t_{\text{cp}}$  determined from TOM measurements, and theoretical values, predicted by F–H equation from the interaction parameters and kinetic equations, at different temperatures and compositions. As can be seen, there is a fine agreement among both data for the temperature range studied.

In a previous paper [15], the phase diagram for DGEBA/DDM/PEO–PPO–PEO system was obtained using this thermodynamic model. Two different behaviours could be

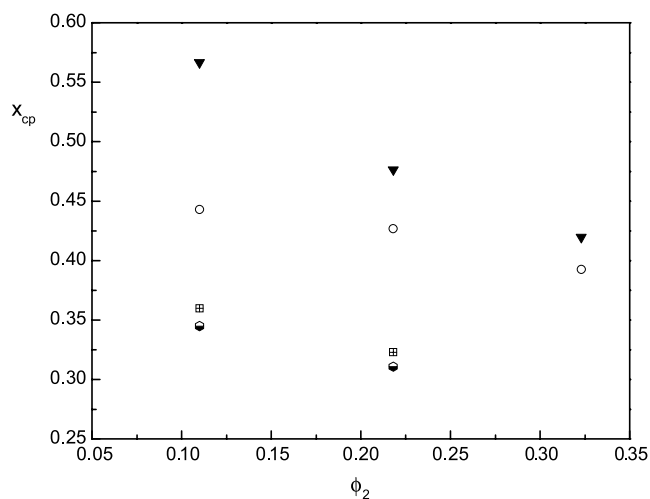


Fig. 4. Cloud-point conversion for DGEBA–DDM system modified with different PEO–PPO–PEO volumetric fractions ( $\phi_2$ ) at: (▼) 140 °C, (○) 150 °C, (■) 160 °C and (●) 170 °C.

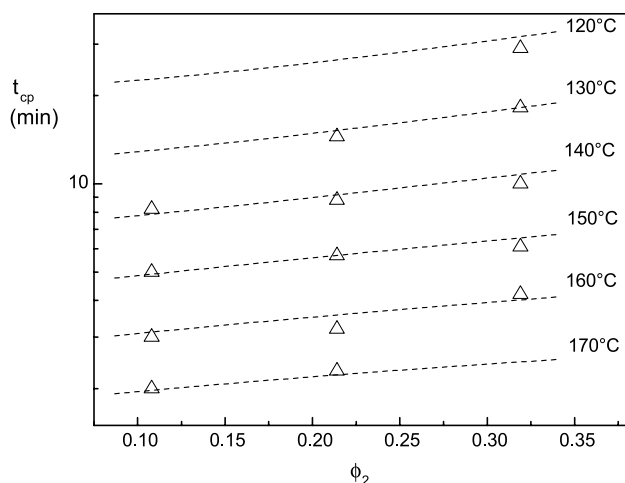


Fig. 5. Experimental ( $\Delta$ ) and predicted cloud-point times (---) for blends modified with several volumetric fractions ( $\phi_2$ ) of PEO–PPO–PEO.

observed depending on curing temperature. At high temperature range, the cloud point conversion of the critical point  $x_c$  is lower than gelation conversion  $x_g$  leading to a micro separated system. For low curing temperatures, however,  $x_c$  increases leading to gelation takes place before micro phase separation can occur [28]. Anyway, phase nanoseparation could occur in the gelation region but it cannot be detected by light transmission analysis, since it is not able to detect particles smaller than 100 nm.

For analysis of phase nanoseparation the competition between kinetic and thermodynamic factors has to be considered. With respect to thermodynamic factors, the contribution of configurational entropy of mixing on free energy of mixing during curing decreases, being the principal driving force for phase separation, whilst the variation of the interaction parameter with conversion is the secondary driving force of phase separation process. At high curing temperatures, as  $x_{cp}$  is lower than  $x_g$ , phase micro separation occurs. At low curing temperatures, however, taking into account the evolution of cloud point conversions upon temperature shown in Fig. 4,  $x_{cp}$  would be higher than  $x_g$ . Thus, phase micro separation is avoided. On the other hand, as cloud point conversions are lower for higher copolymer contents, phase separation could start at gelation or even at higher conversions, thus leading to particles of nanometric size since their growing would not be possible at those high conversions.

### 3.3. Micro structural and dynamic mechanical analysis

AFM scans reveal the presence of two phases for every blends except for the blend containing 10 wt% PEO–PPO–PEO cured at 80 °C. Depending on curing conditions, the separation appears to be at micro or nanoscale.

As it is shown in Fig. 6(a)–(c), for the blends cured at 80 °C the final morphology is very affected by block copolymer content. All blends showed optical transparency.

The blend with 10 wt% remains miscible, however, the blends with 20 and 30 wt% present phase-separated nanosize domains.

Fig. 7(a)–(c) presents the morphologies of blends cured at 140 °C. All blends show spherical domains but the size and content of micro domains change with copolymer content. The blend with 10 wt% PEO–PPO–PEO shows three sizes at around of 140, 400 and 750 nm. The size of micro spheres decreases to 350–500 nm when the copolymer content increases to 20 wt%. The blend containing 30 wt% PEO–PPO–PEO shows an increase in size domains up to 450 and 850 nm.

The blends have also been examined using dynamic mechanical analysis to get more information about microstructure. Figs. 8(a), (b) and 9(a), (b) show the storage modulus and  $\tan \delta$  variation with temperature for DGEBA/DDM modified with 10 and 20 wt%, respectively, of PEO–PPO–PEO, PPO and PEO cured at 80 and 140 °C and postcured at 190 °C. For comparison, the neat DGEBA/DDM system has also been included. For 10 wt% modified system cured at 80 °C, Fig. 8(a), the similar temperature of the  $\alpha$  relaxation of epoxy-rich phase, which appears as a maximum in  $\tan \delta$  curve and a drop of  $E'$ , for PEO–PPO–PEO and PEO (miscible with the epoxy resin [18,29,30]), suggest that gelation occurs before nano or micro separation leading to a miscible system. For high curing temperature (Fig. 8(b)), however, the  $\alpha$  relaxation for PEO–PPO–PEO modified blend appears to be very similar to that for the modified with 10 wt% PPO (micro separated system), thus confirming the microstructure suggested by both opacity and AFM images. This fact outlines the importance of using different techniques for a better understanding of phase separation dynamics.

For 20 wt% PEO–PPO–PEO modified system cured at 80 °C, the  $\alpha$  relaxation appears to be intermediate between the corresponding ones to PPO and PEO modified systems, Fig. 9(a), indicating that the blend of 20 wt% cured at 80 °C leads to nanomorphologies, as above shown in the AFM image. However, for 140 °C a similar behaviour than 10 wt% modified system is observed, Fig. 9(b).

Moreover, Fig. 10(a) and (b) shows DMA curves at low temperatures for systems with both cure cycles used. As can be seen, the systems cured at high temperature present the  $T_g$  of PEO–PPO–PEO around  $-80$  °C at all contents. On the contrary, for the 20 and 30 wt% modified systems cured at low temperature the peak related to this  $T_g$  is not so intense as for the systems with microscopic separation, thus confirming nanophase separated structures. The displacement of this peak to higher temperatures can be related to physical interactions between PEO blocks and epoxy matrix.

Table 3 shows the  $T_g$  of epoxy-rich phase taken as the maximum in the loss factor curves. As it can be seen, for systems cured at 80 °C the  $T_g$  of nanoseparated systems are close to that for 10 wt% modified miscible system. This could be attributed to the fact that a part of copolymer

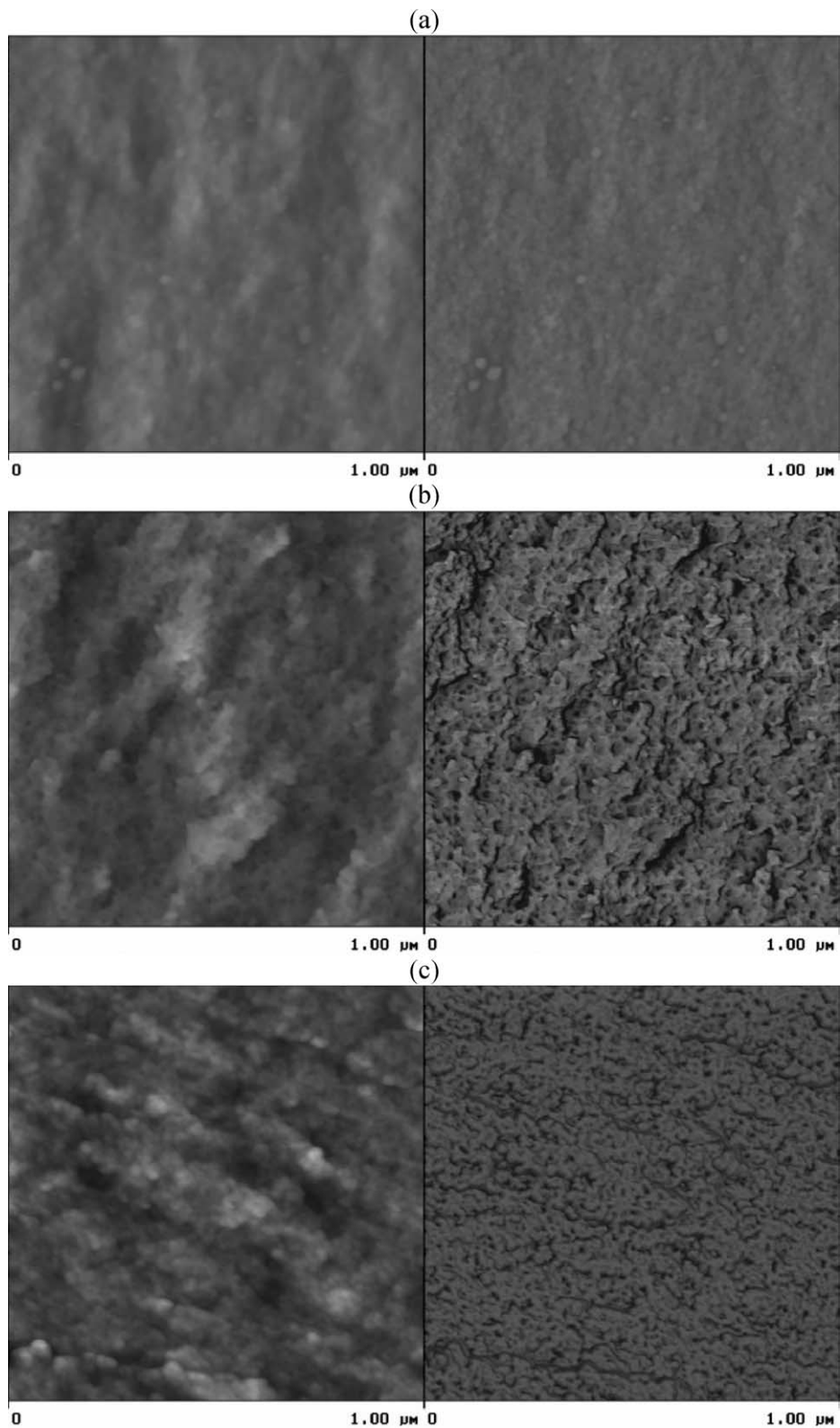


Fig. 6. Tapping mode AFM images of epoxy blends precured at 80 °C and postcured at 190 °C containing several amounts of PEO–PPO–PEO: (a) 10 wt%, (b) 20 and 30 wt%. Topographical (left), and phase images (right).

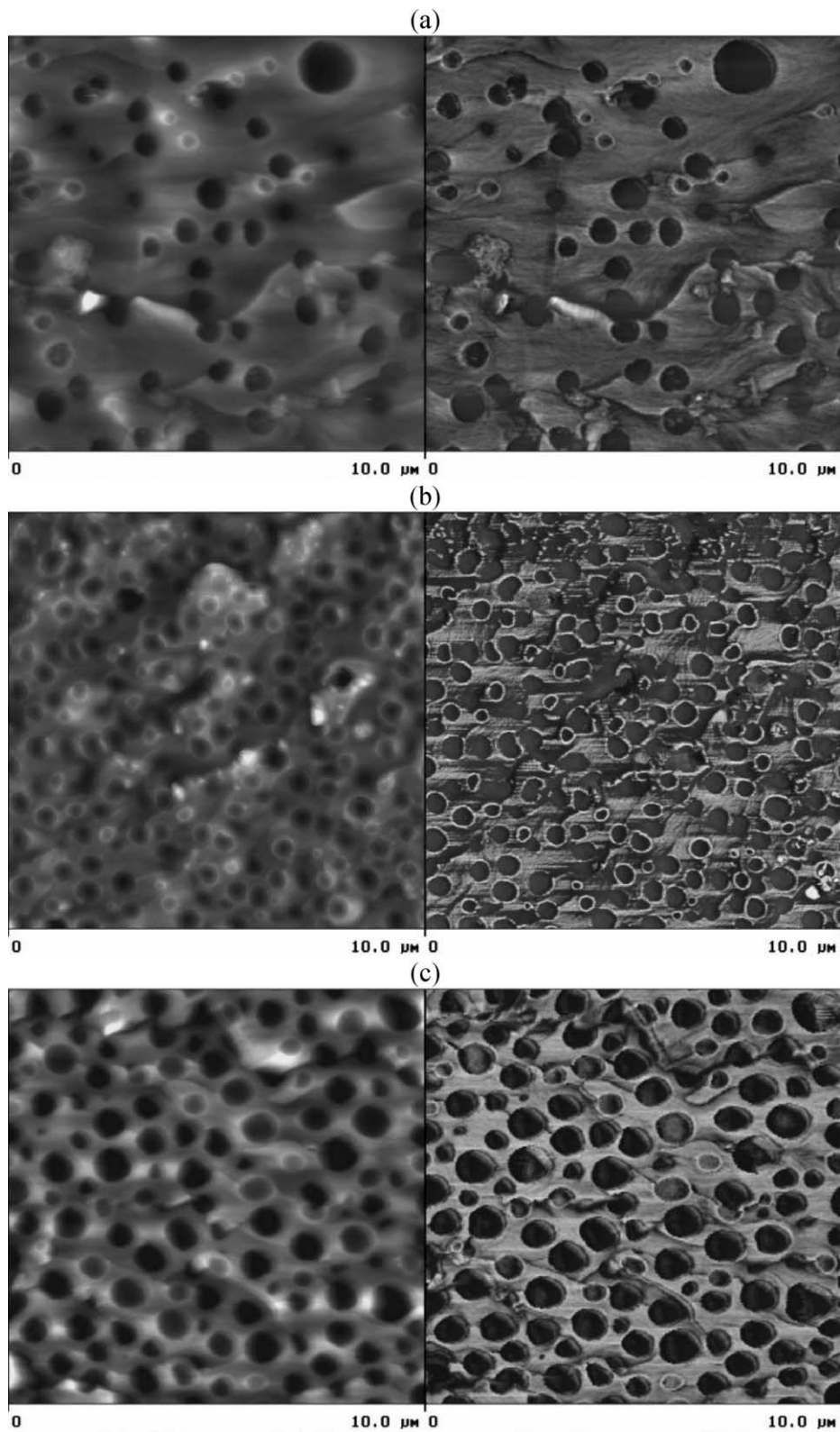


Fig. 7. Tapping mode AFM images of epoxy blends precured at 140 °C and postcured at 190 °C containing several amounts of PEO–PPO–PEO: (a) 10 wt%, (b) 20 and 30 wt%. Topographical (left), and phase images (right).



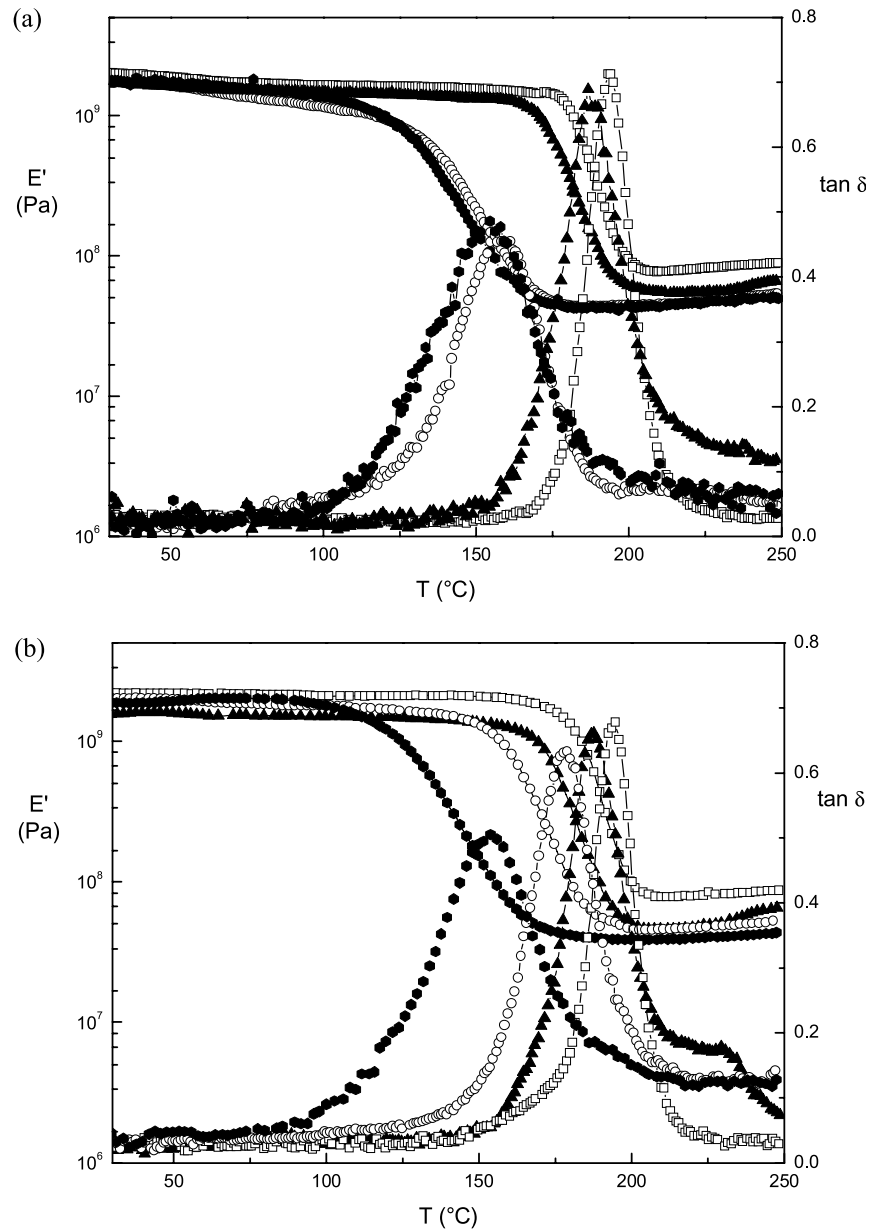


Fig. 8. Storage modulus ( $E'$ ) and loss factor ( $\tan \delta$ ) variation upon temperature for DGEBA/DDM modified with 10 wt% of: (●) PEO, (○) PEO–PPO–PEO, (▲) PPO, and (□) neat matrix, cured at (a) 80 °C, (b) 140 °C, and postcured at 190 °C.

remains miscible. For micro separated systems, however, the  $T_g$  are higher than the corresponding ones for low curing temperature. In addition, the  $T_g$  slightly increases with copolymer content, thus indicating that the content of modifier decreases in epoxy-rich phase. Thus, DMA measurements confirm the results obtained by AFM.

Contradictory results obtained by Mijovic et al. [11] and Guo et al. [12] for the blends used in this study can be explained taking into account competition between thermodynamic and kinetic factors. Mijovic et al. used high curing temperature, where the influence of the thermodynamic factors is higher. However, at low temperature, as seen by Guo et al. the kinetic factor is dominant, gelation occurs

Table 3

Physical structure of different systems and  $T_g$  of epoxy-rich phase as a function of modifier concentration and cure temperature ( $T_{cure}$ )

PEO–PPO–PEO (wt%)	$T_{cure}$ (°C)	Structure	$T_g$ (°C)
0	80	Homogeneous	194
10	80	Homogeneous	159
10	140	Microseparated	178
20	80	Nanoseparated	155
20	140	Microseparated	180
30	80	Nanoseparated	159
30	140	Microseparated	183

All systems have been postcured at 190 °C for 2 h.

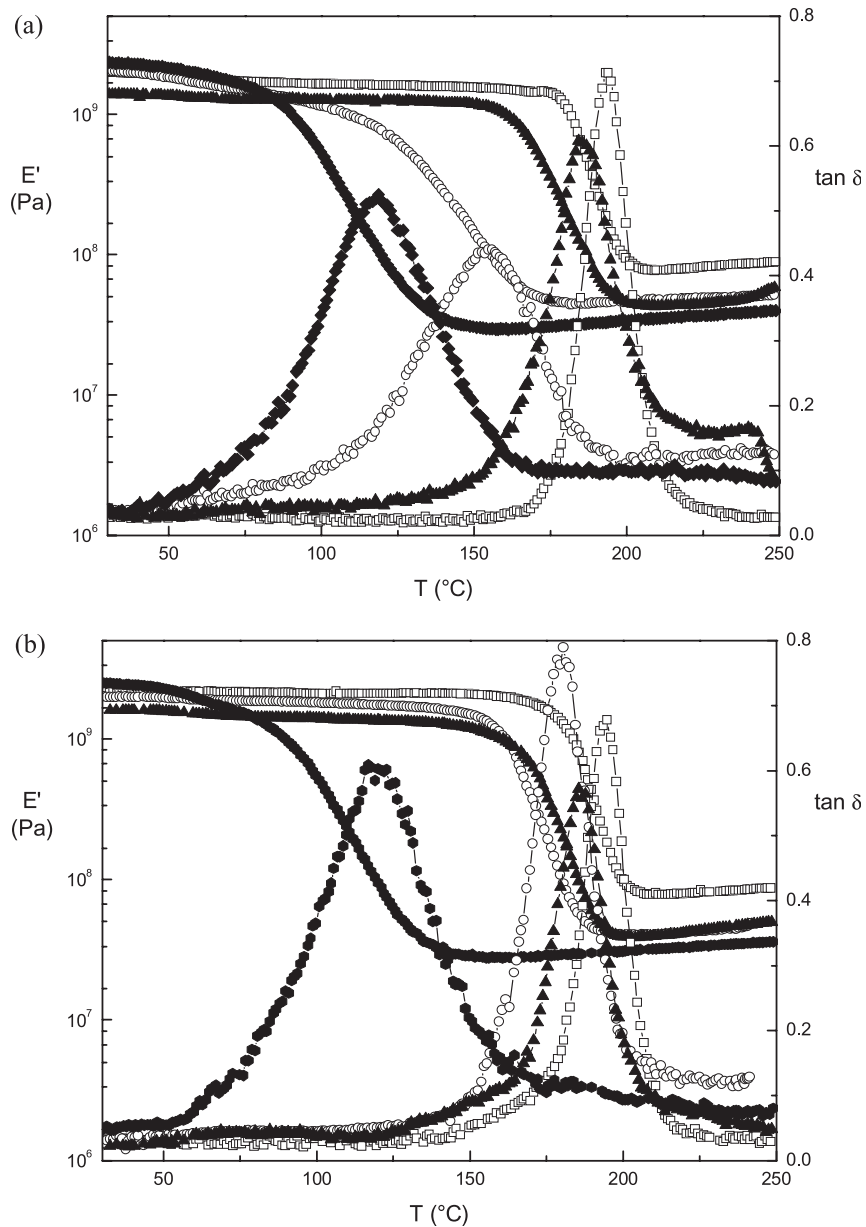


Fig. 9. Storage modulus ( $E'$ ) and loss factor ( $\tan \delta$ ) variation upon temperature for DGEBA/DDM modified with 20 wt% of: (●) PEO, (○) PEO–PPO–PEO, (▲) PPO, and (□) neat matrix, cured at (a) 80 °C, (b) 140 °C, and postcured at 190 °C.

before phase micro separation and nanoseparated structures can be obtained for high contents of copolymer. In addition to curing conditions, the physical characteristics of the block copolymer itself are also important in order to obtain phase nanoseparated systems. This influence will be reported in a future publication.

#### 4. Conclusions

A DGEBA/DDM epoxy blend has been modified with a PEO–PPO–PEO block copolymer at various compositions, ranging from 0 to 30 wt%. Characterization of curing and phase separation by kinetic, thermodynamic and dynamic

mechanical analysis has allowed us to elucidate the miscibility and morphological features of blends for any curing condition.

Depending on the copolymer content and curing temperature, different morphological behaviours can be obtained. At low curing temperature, the obtained materials are optically transparent. However, AFM and DMA analyses revealed that two different phases corresponding to phase nanoseparated structures are present in blends with high copolymer contents. On the contrary, all the systems cured at high temperature are opaque, showing micro dispersed spherical domains.

Phase separation occurring at micro- or nanoscale has been analysed taken into account the competition between

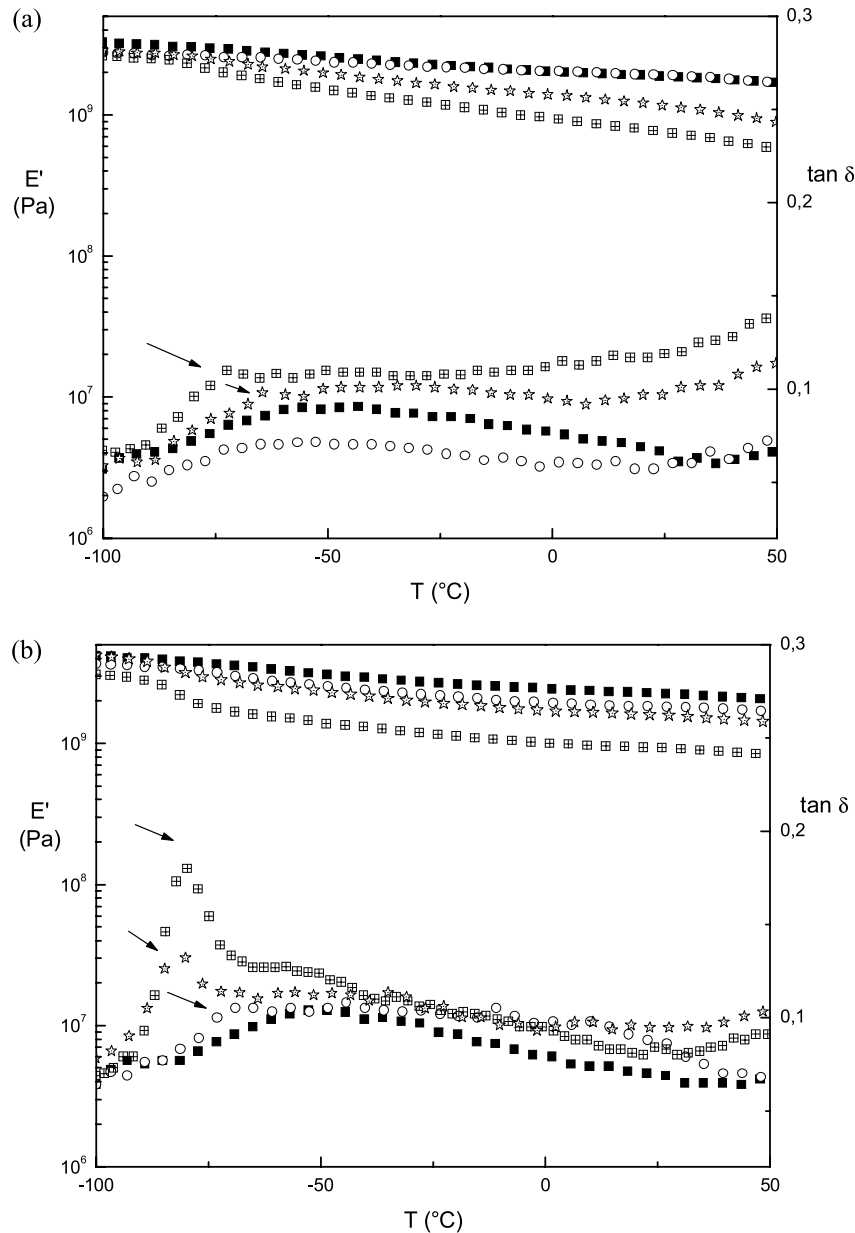


Fig. 10. Storage modulus ( $E'$ ) and loss factor ( $\tan \delta$ ) variation upon low temperature for DGEBA/DDM modified with: (○) 10 wt%, (☆) 20 wt%, (⊞) 30 wt% and (■) neat matrix, cured at (a) 80 °C and at (b) 140 °C, and postcured at 190 °C.

thermodynamic and kinetic factors. Curing kinetics has been analysed by mechanistic approach. Since the modifier delays reaction, it has been proved that the influence of  $K$  and  $K_1$  constants on reaction rate is higher than the influence of  $K'_1$ . Respect to the thermodynamic factor the model used describes a LCST behaviour, which allows to elucidate the different morphologies depending on curing temperature. Cloud point conversion at high curing temperature appears to be lower than that for gelation, thus leading to phase micro separation. Nevertheless, at low curing temperature gelation takes place before cloud point conversion is reached. At these conditions, blend remains miscible at low copolymer contents. At high contents, however, due to

the decrease of cloud point conversion, phase separation starts at gelation or even at higher conversions thus resulting in phase nanoseparated structures.

#### Acknowledgements

Funding for this work was provided by Ministerio de Ciencia y Tecnología (Spain) Grants MAT2000-0293 and MAT2001-0714. M. Larrañaga acknowledges financial support (grant for PhD) from the Ministerio de Ciencia y Tecnología (MAT1998-0656). C.C. Riccardi also thanks to Gobierno Vasco/Eusko Jaurlaritza for its financial support.

## References

- [1] Hillmyer MA, Lipic PM, Hajduk DA, Almdal W, Bates FS. *J Am Chem Soc* 1997;119:2749–50.
- [2] Lipic PM, Bates FS, Hillmyer MA. *J Am Chem Soc* 1998;120: 8963–70.
- [3] Urbas A, Fink Y, Thomas EL. *Macromolecules* 1999;32:4748–50.
- [4] Girard-Reydet E, Sautereau H, Pascault JP, Keates P, Navard P, Thollet G, et al. *Polymer* 1998;39:2269–80.
- [5] Schauer E, Berglund L, Peña G, Marieta C, Mondragon I. *Polymer* 2002;43:1241–8.
- [6] Chen W, David DJ, MacKnight JW, Karasz FE. *Macromolecules* 2001;34:4277–84.
- [7] Barral L, Cano J, Díez FJ, López J, Ramírez C, Abad MJ, Ares A. *J Polym Sci, Part B: Polym Phys* 2002;40:284–9.
- [8] Dean JM, Lipic PM, Grubbs RB, Cook RF, Bates FS. *J Polym Sci, Part B: Polym Phys* 2001;39:2996–3010.
- [9] Grubbs RB, Dean JM, Broz ME, Bates FS. *Macromolecules* 2000;33: 9522–34.
- [10] Guo Q, Thomann R, Gronski W, Staneva R, Ivanova R, Stühn B. *Macromolecules* 2003;36:3635–45.
- [11] Mijovic J, Shen M, Sy JW, Mondragon I. *Macromolecules* 2000;33: 5235–44.
- [12] Guo Q, Thomann R, Gronski W, Thurn-Albrecht T. *Macromolecules* 2002;35:3133–44.
- [13] Ritzenthaler S, Court F, David L, Girard-Reydet E, Leibler L, Pascault JP. *Macromolecules* 2002;35:6245–354.
- [14] Ritzenthaler S, Court F, Girard-Reydet E, Leibler L, Pascault JP. *Macromolecules* 2003;36:118–26.
- [15] Larrañaga M, Martín MD, Gabilondo N, Kortaberria G, Corcuera MA, Riccardi CC, et al. *Polym Int* 2004;53:1495–502.
- [16] Riccardi CC, Fraga F, Dupuy J, Williams RJJ. *J Appl Polym Sci* 2001; 82:2319–25.
- [17] Gyrard-Reydet E, Riccardi CC, Sautereau H, Pascault JP. *Macromolecules* 1995;28:7599–607.
- [18] Guo Q, Harrats C, Groeninckx G, Koch MHJ. *Polymer* 2001;42: 4127–40.
- [19] Remiro PM, Riccardi CC, Corcuera MA, Mondragon I. *J Appl Polym Sci* 1999;74:772–80.
- [20] Flory PJ. *Principles of polymer chemistry*. Ithaca, New York: Cornell University Press; 1953.
- [21] Riccardi CC, Borrajo J, Williams RJJ, Gyrard-Reydet E, Sautereau H, Pascault JP. *J Polym Sci, Part B: Polym Phys* 1996;34:349–56.
- [22] Stockmayer WH. *J Polym Sci* 1952;9:69–71.
- [23] Stockmayer WH. *J Polym Sci* 1953;11:424.
- [24] Riccardi CC, Borrajo J. *Polym Int* 1993;3:241–6.
- [25] Riccardi CC, Borrajo J, Maynie L, Fenouillot F, Pascault JP. *J Polym Sci, Part B: Polym Phys* 2004;42:1351–60.
- [26] Bonnaud L, Bonnet A, Pascault JP, Sautereau H, Riccardi CC. *J Appl Polym Sci* 2002;83:1385–96.
- [27] Williams RJJ, Rozenberg BA, Pascault JP. *Adv Polym Sci* 1997;128: 95–156.
- [28] Girard-Reydet E, Sautereau H, Pascault JP, Keates P, Navard P, Thollet G, et al. *Polymer* 1998;39:2269–80.
- [29] Zheng S, Zhang N, Luo X, Ma D. *Polymer* 1995;36:3609–13.
- [30] Guo Q. In: Shonaike GO, Simon G, editors. *Polymer blends and alloys*. New York: Marcel Dekker; 1999.